BMC Microbiology

RESEARCH

Open Access

Identification of hub genes and potential networks by centrality network analysis of PCR amplified *Fusarium oxysporum* f. sp. *lycopersici* EF1α gene

Yashoda N. Tripathi[1*], Vinay K. Singh[2], Sunil Kumar[1], Vaishali Shukla[1], Mukesh Yadav[1] and Ram S. Upadhyay[1]

Abstract

Background Fusarium wilt is a devastating soil-borne fungal disease of tomato across the world. Conventional method of disease prevention including usage of common pesticides and methods like soil solarisation are usually ineffective in the treatment of this disease. Therefore, there is an urgent need to identify virulence related genes in the pathogen which can be targeted for fungicide development.

Results Pathogenicity testing and phylogenetic classification of the pathogen used in this study confirmed it as *Fusarium oxysporum* f. sp. *lycopersici* (Fol) strain. A recent discovery indicates that EF1α, a protein with conserved structural similarity across several fungal genera, has a role in the pathogenicity of *Magnaporthe oryzae*, the rice blast fungus. Therefore, in this study we have done structural and functional classification of EF1α to understand its role in pathogenicity of Fol. The protein model of Fol EF1α was created using the template crystal structure of the yeast elongation factor complex EEF1A:EEF1BA which showed maximum similarity with the target protein. Using the STRING online database, the interactive information among the hub genes of EF1α was identified and the protein–protein interaction network was recognized using the Cytoscape software. On combining the results of functional analysis, MCODE, CytoNCA and CytoHubba 4 hub genes including Fol *EF1α* were selected for further investigation. The three interactors of Fol EF1α showed maximum similarity with homologous proteins found in *Neurospora crassa* complexed with the known fungicide, cycloheximide. Through the sequence similarity and PDB database analysis, homologs of Fol EF1α were found: EEF1A:EEF1BA in complex with GDPNP in yeast and EF1α in complex with GDP in *Sulfolobus solfataricus*. The STITCH database analysis suggested that EF1α and its other interacting partners interact with guanosine diphosphate (GDPNP) and guanosine triphosphate (GTP).

Conclusions Our study offers a framework for recognition of several hub genes network in Fusarium wilt that can be used as novel targets for fungicide development. The involvement of EF1α in nucleocytoplasmic transport pathway suggests that it plays role in GTP binding and thus apart from its use as a biomarker, it may be further exploited as an effective target for fungicide development. Since, the three other proteins that were found to be tightly associated Fol EF1α have shown maximum similarity with homologous proteins of *Neurospora crassa* that form complex with fungicide- Cycloheximide. Therefore, we suggest that cycloheximide can also be used against Fusarium wilt disease in tomato. The active site cavity of Fol EF1α can also be determined for computational screening of fungicides

*Correspondence:
Yashoda N. Tripathi
tn.yashoda@gmail.com
Full list of author information is available at the end of the article

using the homologous proteins observed in yeast and *Sulfolobus solfataricus*. On this basis, we also suggest that the other closely associated genes that have been identified through STITCH analysis, they can also be targeted for fungicide development.

Keywords Centrality analysis, Hub geness, Protein–protein interactions, *Fusarium oxysporum* f. sp. *lycopersici*, Tomato, Elongation factor 1α

Background

Fusarium oxysporum (FO) is a filamentous, asexual fungus that causes several diseases like root rot, wilting and necrosis in a large number of host plants. Fusarium wilt (FW) disease is one of the most devastating diseases of tomato. A soil-inhabiting fungus *Fusarium oxysporum* f. sp. *lycopersici* (Fol) is the causal organism of this disease which is very prominent in temperate countries like USA where it is most severe in central and southern states [1] and majorly infects the tomato plants grown in greenhouse and field conditions [2]. The primary symptoms of this disease include yellowing and wilting of leaves with little to no crop production. The disease related yield loss may range between be 30 to 40% and under favourable weather conditions, this may reach up to 80% [2, 3]. It has been ranked as the fifth most important plant pathogen of scientific/economic importance [4, 5]. The Fol–tomato pathosystem is the most studied, and is considered as the best model system to study the molecular mechanisms underlying plant disease and resistance [6]. During infection, Fol invades the root epidermis and colonizes the vascular tissue by producing mycelium and conidia [2, 7, 8]. The development of apparent wilt symptoms results from the clogging of xylem vessels, which obstruct the vasculature and prevents the transport of water and nutrients [7].

For management and control of wilt disease it is important that *Fusarium* isolates are quickly and accurately identified. Although, ITS (Internal Transcribed Spacers) is a suitable DNA barcoding marker for fungal identification, it does not work well with a highly speciose genera like *Fusarium* due to narrow or no barcode gap in their ITS region [9]. For species-level identification, the translation elongation factor 1α (*EF1α*) gene has been widely used in the taxonomy and systematics of the genus *Fusarium* [10, 11]**.** This gene is regarded as the most suitable for *Fusarium* metabarcoding methods due to its phylogenetic utility and the fact that this organism has only a single copy of it.

Functionally, elongation factors in bacteria (EF-Tu, also referred to as Ef1α), and in eukaryotes (the eukaryotic Elongation Factor 1 Complex [eEF1α]), transfers aminoacylated tRNAs to the ribosome during protein translation [12]. However, in bacteria, EF-Tu is also associated with virulence in both Gram-positive and Gram-negative pathogenic bacteria [13] leading to the usage of selective antibiotics (elfamycins) as therapeutic target against EF-Tu since the 1970s [14, 15]. Similarly, in eukaryotes several moonlighting or secondary functions of EF1α have been well established [16–20]. For instance, in the context of plant pathogenesis, a recent work on *Magnaporthe oryzae* the cause of rice blast disease, it was demonstrated that Ebg1 and EF1α interact to evade β-1,3-glucan-triggered host immunity during infection [21]. Ebg1 is an exo-β-1,3-glucanase of the GH17 family that acts as a pathogen-associated molecular pattern (PAMP) to elicit an immune response in the host. However, the interaction with EF1α masks the ability of the host to detect Ebg1 as a PAMP. It can thus be speculated that *EF1α* is a novel gene in fungi that contributes to pathogenicity. Given the conserved structural similarity of EF1α amongst different genera of fungi, in addition to structural similarity between *M. oryzae* and *Fusarium graminearum* Ebg1, it is highly probable that this interaction also contributes to pathogenicity of *Fusarium* in tomato wilt disease. Hence, the sequential and structural classification of EF1α protein of Fol is important to elucidate its functional information and particularly its role in Fol pathogenicity.

The functional association of partner genes of *EF1α* gene can be studied using bioinformatics approaches like Protein–protein interactions (PPIs) networking and by discovering the protein/chemical interactors. PPIs, the actual physical links between two or more proteins are a representation of intricate biological processes. Currently, PPIs are utilised to build PPI networks to analyse complex pathways and uncover the activities of unidentified proteins [22]. PPIs are thought to be involved in many complex biological processes such as metabolic pathways and signalling cascades, therefore it is very important to study the nature of these interactions [23, 24].

In the current study, we have used computational functional genomics methods to elucidate functional information based on the sequential and structural classification of *EF1α* gene. In order to find the novel cluster and putative hub genes linked to Fusarium wilt *EF1α*, we have performed cluster and centrality analyses (Fig. 1).

Materials and methods

Fungal strains, culture condition and pathogenicity test

The experimental fungus Fol strain MTCC10270 obtained from Microbial Type Culture Collection, Institute of Microbial Technology (IMTECH), Chandigarh, India was routinely maintained in potato dextrose agar (PDA) medium

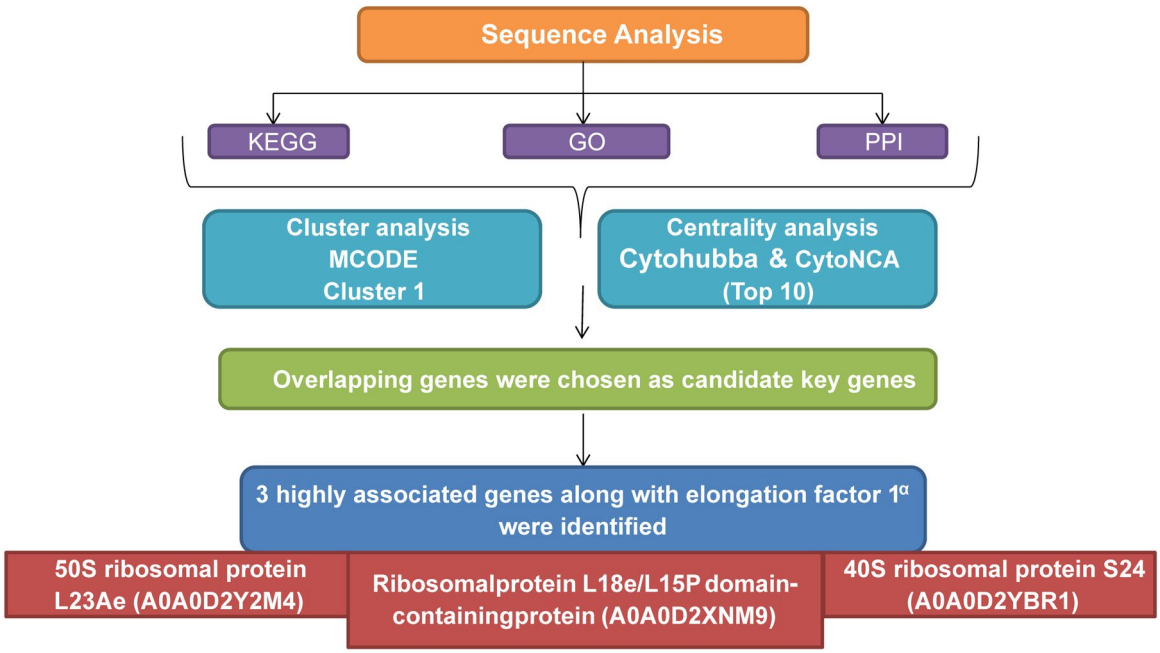

Fig. 1 Study design flowchart

in 90 mm diameter petri dishes and grown at 25 ± 2 °C in the dark. It was given a code name as FUSOX_AT. Seeds of tomato cv. Sel 7, which has been previously reported to be susceptible to Fusarium wilt [25] was provided by the Indian Institute of Vegetable Research (IIVR), Varanasi, India. These seeds were used for the virulence analysis of the Fol strain.

Pathogenicity analysis was carried out using the standard root dip approach. The spore suspension used for inoculation was prepared from a 7 days-old culture and was applied at a concentration of 1×10^7 spores/ml [26]. Tomato seedlings that were 14 days old were delicately pulled while maintaining the integrity of the roots. After trimming the root apex (approximately 1 cm) with sterile scissors, the roots were submerged in the spore suspension for two hours [27]. The inoculated seedlings and control plants were then transplanted into minipots (10 cm in diameter, 0.1% mercuric chloride surface sterilised), which contained sterilised soil and sand in a 1:1 ratio. Henceforth, the plants were watered twice daily with not more than 30% moisture. As a control, non-inoculated tomato plants were used. The experiment was conducted in triplicate.

Molecular characterisation of the fungus

DNA extraction

The Fol isolate was cultivated on PDA medium for 5 days at 25 ± 2 °C, and then approximately 100 mg of mycelium was used for DNA extraction using the cetyltrimethyl ammonium bromide (CTAB) method [28]. The quality and quantity of DNA was estimated on 1% agarose gel as well as by using a ND-1000 spectrophotometer (Thermo Fisher Scientific Inc., Wilmington, DE, United States). DNA sample was diluted to a concentration approximately 20 ng/mL and stored at -20° C for further use.

PCR conditions

The translation *EF1α* gene was amplified for the molecular analysis using primers ef1 (5'- ATGGGTAAGGAA GACAAGAC-3') and ef2 (5'-GGAAGTACCAGTGAT CATGTT-3') [29, 30]. PCR reaction was conducted in a 25 µL final volume. The reaction mixture comprised of 1.0 µL of DNA template, 2.0 µL of 10X PCR buffer (Mg^{2+} included),0.5 µL of $MgCl_2$, 0.25 µL of Taq polymerase (2.5 U/mL), 0.5 µL of deoxynucleotide triphosphate (dNTPs) (2.5 mM each), 1.0 µL forward and reverse primers (10 mM), and 18.75 µL MQ H_2O. The amplification reactions were conducted in a Takara Thermal Cycler (TP600), using conditions specific for *EF1α* gene. PCR cycling protocol for the amplification of *EF1α* gene was as follows: an initial preheating at 95°C for 3 min, followed by 30 cycles of denaturation at 95°C for 30 s, annealing at 58°C for 30 s and extension at 72°C for 45 s, followed by one cycle of final extension at 72°C for 10 min.

Amplicon sequencing, sequence analysis and phylogeny

ABI 3730xl DNA analyzer (Applied Biosystems, Foster City, CA, United States) was used for the Sanger sequencing. The sequence similarity was matched with available FO (taxid:5507) sequence datasets in GenBank using BLAST (http://www.ncbi.nlm.nih.gov/). Full-length *EF1α* sequence

was used as query in the BLAST analysis to find similarities to published sequences. The sequence of FUSOX_AT (MTCC10270) obtained in the current study was uploaded to GenBank. The NCBI GenBank database was utilised to download the *EF1α* sequences of the FUSOX_AT and FO strains from various formae speciales, which were then used as reference sequences in the phylogenetic analysis. These nucleotide sequences were aligned with ClustalW using the Molecular Evolutionary Genetics Analysis software package, version 11 (MEGA 11) [31]. A UPGMA tree was constructed using the maximum composite likelihood method. Bootstrap analysis with 1000 replications was taken to assess group support with tree topology. Branch length was proportional to the number of nucleotide changes (bar).

Full length protein sequence retrieval

Basic Local Alignment Search Tool (BLAST) which is a sequence similarity search program [32, 33] was used to retrieve the complete protein sequence, which showed 100% similarity to the protein sequence of ON871818.1. It was taken for further structure modelling and validation.

Structure modelling and validation

BIOVIA Discovery Studio 2019 was used for structure prediction and PDBsum server was used for PROCHECK analysis which checks the stereo-chemical quality of a protein structure [34].

Protein–protein interaction analysis and hub genes identification

We constructed a PPI network using online STRING database (https://cn.string-db.org/) [35]. The minimum required interaction score was medium confidence (0.400). Cytoscape software (version 3.8.0) was used to construct the PPI network and analyze the hub genes [36]. The Molecular COmplex DEtection (MCODE) algorithm, which is a plugin in Cytoscape was then used to construct the subnetwork and the highly coupled clusters in the PPI network. The criteria for the MCODE analysis parameter setting: degree cut off=2, MCODE scores>5, max depth=100, k-core=2, and node score cutoff=0.2. Finally, CytoHubba (version 0.1) and and CytoNCA (version 2.1.6) which are two other Cytoscape plug-ins were used to detect the top 10 hub genes [37]. The top 10 hub genes in the network were ranked by MCC method.

Protein-chemical interaction analysis using STITCH server

STITCH server was used to check associations between chemicals and proteins [38]. Using the STITCH database (stitch.embl.de/cgi), predicted protein targets were retrieved and a protein-chemical interaction (PCI) network was constructed. Functional enrichment, including biological processes and KEGG pathways of the network were analysed using the STITCH database.

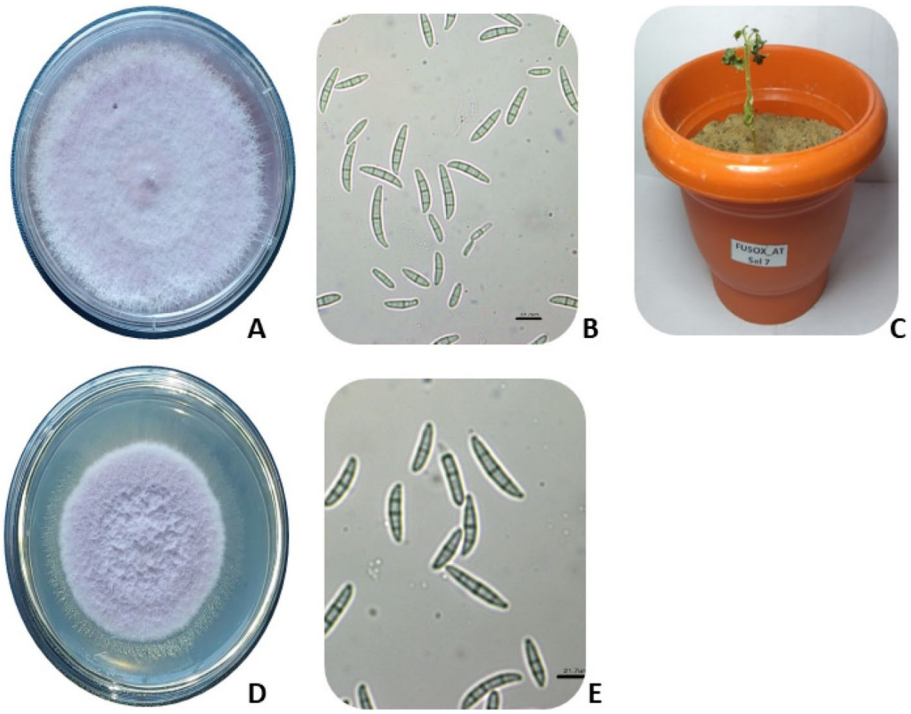

Fig. 2 Pathogenicity test. **A** Colony of Fol on PDA plate (**B**) Conidia of Fol as observed at 40X (**C**) Symptoms on infected tomato plant (**D**) Pure colony of Fol re-isolated from infected tomato plant on PDA plate (**E**) Conidia of re-isolated Fol as observed at 40X

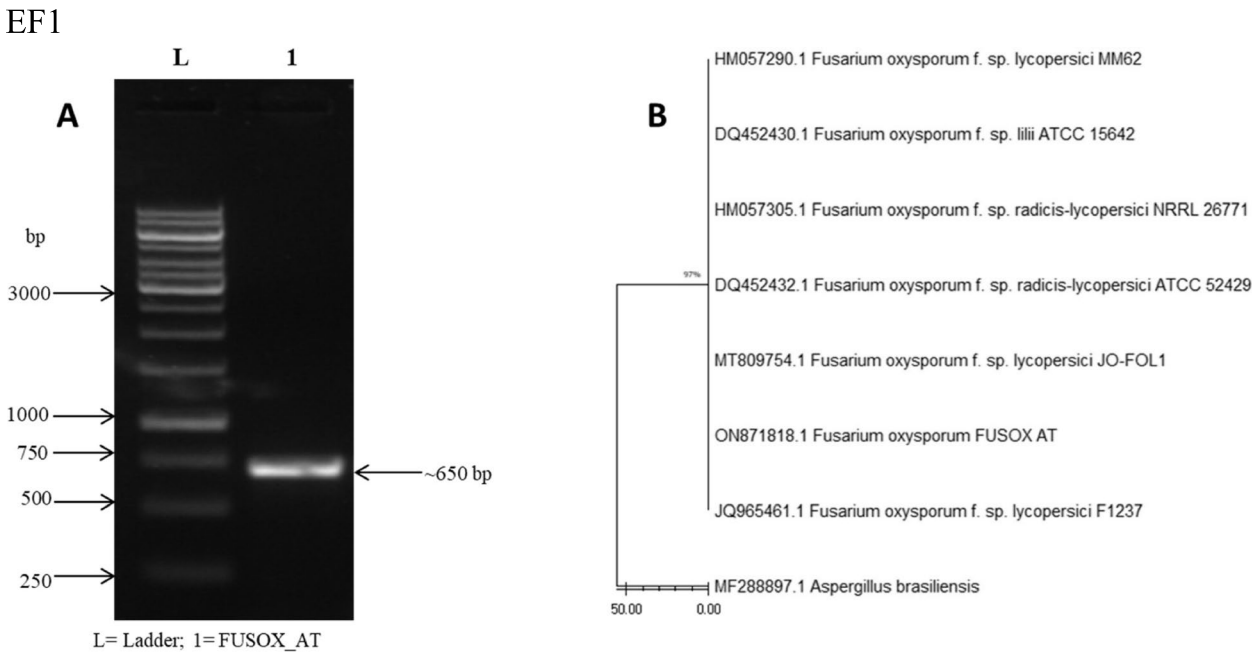

Fig. 3 Gel electrophoresis and phylogenetic analysis of Fusarium strain based on EF1α sequence. **A** Gel electrophoresis of the PCR product with primers, ef1/ef2 of DNA from the Fol culture. Lane L, molecular weight markers (1 kb ladder); lane 1, *Fusarium oxysporum* f. sp. *lycopersici* (647 bp). **B** Phylogenetic tree on a fungal strain, the *Fusarium oxysporum* f. sp. *lycopersici*, based on the 18S rDNA gene sequence. A boot strap consensus tree was drawn by multiple sequence alignment using UPGMA method

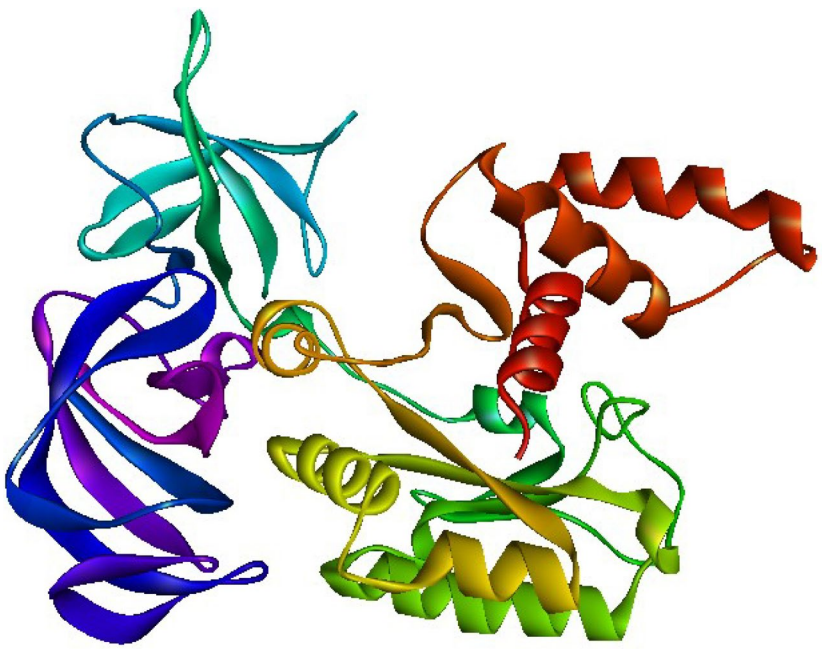

Fig. 4 Homology model prediction of *Fusarium oxysporum* elongation factor 1α using BIOVIA Discovery Studio 2019 based on Yeast EF1α (PDB ID: 1F60_A) as a template

Table 1 Details of predicted models

Number of Atoms	Molecular Formula	Molecular Composition	Molecular Weight	Exact Mol. Weight	Net Formal Charge	PDF Total Energy	PDF Physical Energy	DOPE Score	RMSD	NOverlap	Resolution
3254	C2070 H3318 N562 O606 S16	C: 0.537, H: 0.072, N: 0.170, O: 0.209, S: 0.011	46289.4	46258.2	8	1887.2	1188.03	-47020.4	0.242	424	1.67
						2059.58	1208.39	-47021	0.237	424	
						2065.97	1224.03	-46514.5	0.204	424	
						2102.21	1227.73	-46986.6	0.191	424	
						2122.72	1206.23	-47019.9	0.242	424	

Results

Pathogenicity test

The pathogenicity study showed that after 7 days of inoculation with FUSOX_AT, the symptoms of wilting began to manifest in the treated tomato plants (Fig. 2). The symptoms included: the initial appearance of slight vein clearing on the outer-portion of younger leaves; progression towards epinasty in the older leaves and stunting of the plants; lower leaves showed yellowing; defoliation; marginal necrosis of the rest of the leaves; and finally, the death of the entire plant.

Molecular characterization of the pathogen

The molecular identification of the fungal strain was based on *EF1α* gene amplification and sequencing. The 647 bp partial sequence of *EF1α* gene was submitted to National Centre for Biotechnology Information (NCBI) gene bank database as *Fusarium oxysporum* isolate FUSOX_AT (GenBank accession no. ON871818.1). The phylogenetic analysis by using UPGMA method showed that the FO isolate FUSOX_AT was found together with *Fusarium oxysporum* f. sp. *lycopersici* F1237 (JQ965461.1) in the same clade as shown in Fig. 3.

Structure modelling and validation

Homology modelling

After BlastP analysis, full length EF1α was identified in *Fusarium oxysporum* f. sp. *lycopersici* 4287 with accession number XP_018237716.1 (FASTA sequence Supplementary Info File 1). The homology model for Fol EF1α (XP_018237716.1) was constructed using Yeast EF1α (PDB ID: 1F60_A) as a template, with a sequence identity of 83.18% and query coverage of 95% (Fig. 4). The protein sequences of Fol EF1α /Yeast EF1α were aligned using ClustalW. Further, the homology model generated by BIOVIA was selected based on the lowest DOPE score value. The DOPE score for Fol EF1α was -47020.4 (Table 1). When the sequence was aligned to template in the BIOVIA, the sequence identity was found to be 77.3% and the sequence similarity was 85.6%.

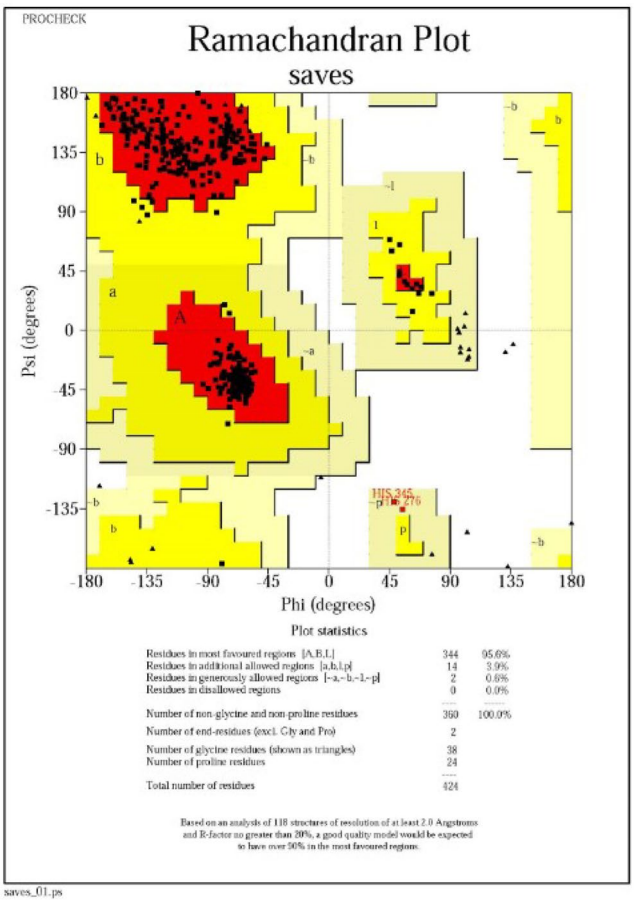

Fig. 5 Ramachandran plot determined by PROCHECK. The regions in the red indicates favoured region, yellow shows allowed region, light yellow indicate generously allowed region of amino acid and white region indicate disallowed region

Evaluation of model quality

The model with the lowest DOPE score was selected and subjected for quality evaluation. The quality of the predicted model was evaluated using PROCHECK. The Ramachandran plot analysis for Fol Ef1α model showed that most of the residues are in the favourable zones i.e. the allowed regions. 95.6% residues are in the most favoured region, 3.9% residues are in additionally allowed region and 0.6% are in generously allowed region (Fig. 5). Further model validation was also carried out using PROCHECK based G-factors that indicates the quality of covalent and bond-angle distance. The Gfactors, indicating the quality of covalent and bond angle distance, were 0.06 for dihedrals, -0.12 for covalent, and overall -0.01 for Fol EF1α. The planar groups were 100% within the limits for Fol EF1α. The overall main-chain and sidechain parameters as evaluated by PROCHECK were favourable for Fol EF1α.

Protein–protein interaction analysis and hub genes identification

The interactive information among hub genes and the PPI network was obtained using the STRING online database (Fig. 6). The details of the homologous sequence (A0A0C4DHQ7) with 100% identity are mentioned in Table 2 (Supplementary Info file 2). The PPI network at a combined score > 0.9 (high confidence interaction score) consisted of 44 nodes and 625 edges visualized with Cytoscape, (Fig. 7a). Finally, imported and interacted proteins were used for further analysis. The Cytoscape software was used to see the association among the selected candidate proteins using its plug-ins MCODE, CytoHubba and CytoNCA. MCODE clusters in a protein–protein interaction network are usually the protein complexes and components of pathways. The CytoNCA and the CytoHubba are two Cytoscape plug-ins for

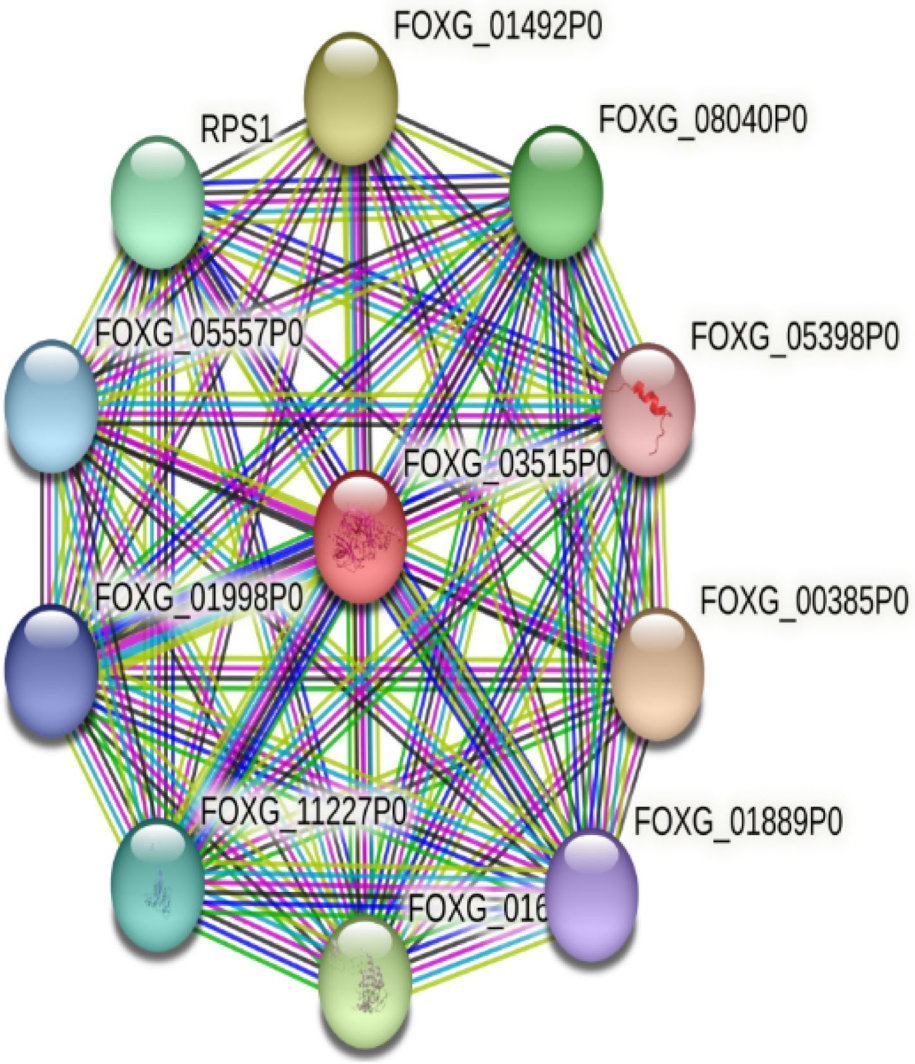

Fig. 6 Protein–protein functional association network using STRING server

Table 2 Homology search details with STRING database for protein–protein functional association

Protein	Organism	Annotation	Identity	Bitscore	e-value
A0A0C4DHQ7	*Fusarium oxysporum* f. sp. *lycopersici* 4287	Elongation factor 1-alpha; This protein promotes the GTP-dependent binding of aminoacyl- tRNA to the A-site of ribosomes during protein biosynthesis	100.00%	885.2	1E-257

centrality analysis and give information about the most influential nodes or edges in a network. The MCC approach has been found to be the most accurate at predicting important proteins from PPI networks among the 11 topological analysis methods offered by CytoHubba, based on short paths [37]. CytoNCA supports eight different centrality measures and helps in detecting specific nodes by integrating biological data with topological data and also by using it, centrality can be calculated with ease. It is an excellent tool for evaluating and visualizing biological networks [39].

Network nodes (colored circles) represent query proteins or first shell of interactors, with a single node representing all the proteins produced by a single protein coding gene. Colored lines between the nodes (edges) represent protein–protein associations evidenced by fusion of genes (red line), neighborhood of genes (green line), gene co- occurrence (blue line), from curated database (sky blue) experimentally determined (purple line), text mining of abstracts from literature (yellow line), protein homology (light blue line), co-expression in the same or others species (black line). Based on the MCODE scoring system a cluster consisting of 35 nodes was screened with a net score cut-off = 0.2 and k-core = 2 (Fig. 7b). We ran CytoHubba application and extracted data from MCC (Maximal Clique Centrality) calculation method. The top 10 nodes ranked by this method were selected (Supplementary Info file 3). Moreover, in CytoNCA application, applying all centralities (without weight) approach the top 10 proteins, including A0A0C4DHQ7 (Elongation factor 1-alpha), A0A0D2Y2M4 (50S ribosomal protein L23Ae), A0A0D2XVM8 (60S ribosomal protein L3),

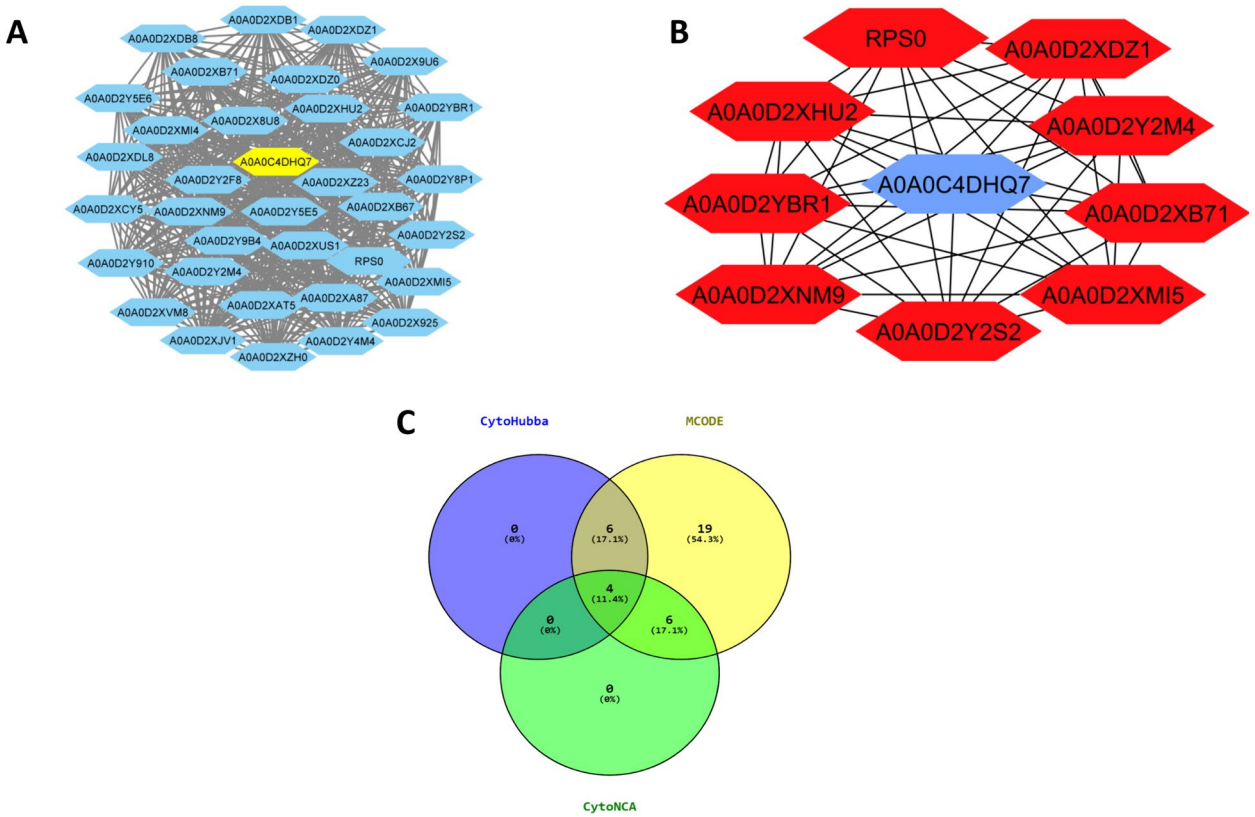

Fig. 7 PPI network and identification of cluster and hub genes. **A** Cluster analysis includes 35 nodes and 539 edges identified using MCODE module of Cytoscape software (**B**) Hub genes were calculated by CytoHubba using MCC method (**C**) A Venn diagram of 4 overlapping genes between different calculation methods of Cytohubba, MCODE and CytoNCA. PPI, protein–protein interaction

A0A0D2XCJ2 (50S ribosomal protein L4e), A0A0D2Y8P1 (40S ribosomal protein S23), A0A0D2X8U8 (60S ribosomal protein L11), A0A0D2Y4M4 (40S ribosomal protein S2), A0A0D2YBR1 (40S ribosomal protein S24), A0A0D2XA87 (Ribosomal protein L15) and A0A0D2XNM9 (Ribosomal protein L18e/L15P domain-containing protein) were obtained (Supplementary Info file 4). Besides, a Venn diagram was created using Venny 2.1.0 to identify the significant hub genes which were showing similarity (Fig. 7c).

Protein-chemical interaction analysis

Using the STITCH database, the functional partners of EF1α were analysed, which resulted in 8 candidate proteins viz. zinc-finger protein zpr1 (FOXB_06147), elongation factor 2 (FOXB_06787), eukaryotic peptide chain release factor subunit 1(FOXB_17523), elongation factor 1-beta (FOXB_02170), hypothetical protein similar to elongation factor 1-gamma 2(FOXB_14687), 116 kDa U5 small nuclear ribonucleoprotein component (FOXB_06716), hypothetical protein similar to elongation factor 2 (FOXG_06276), hypothetical protein similar to cpc-3 protein (FOXB_08906) along with two known chemicals, guanosine diphosphate (GDPNP) and guanosine triphosphate (GTP) (Fig. 8).

In addition, the protein EF1α is involved in Nucleocytoplasmic transport pathway (https://www.genome.jp/dbget-bin/www_bget?fox:FOXG_03515) (Fig. 9). The regulation of nucleocytoplasmic transport, through its influence on gene expression, signal transduction, and development, has been previously reported to play a significant role in disease development in eukaryotes [40]. Overall, these results indicate the role of EF1α in GTP binding (GO:0005525), GTPase activity, translation elongation factor activity and protein biosynthesis and as a potential marker [41]. Statistical significance through clustering and hub gene analysis was successfully conducted and protein–protein/chemical details (coexpression, experimentally determined interaction, database annotated, automated text mining and combined score) are reported in Table 3.

Discussion

Fusarium wilt is a common disease in tomato. The conventional methods of chemical control and soil solarisation are ineffective in control of this disease. Therefore, it is very important to find out the genes responsible for disease progression so that fungicides can be designed and targeted against these genes in order to prevent the wilt disease development in tomato [42]. In the present work, using in silico approach, we have established the

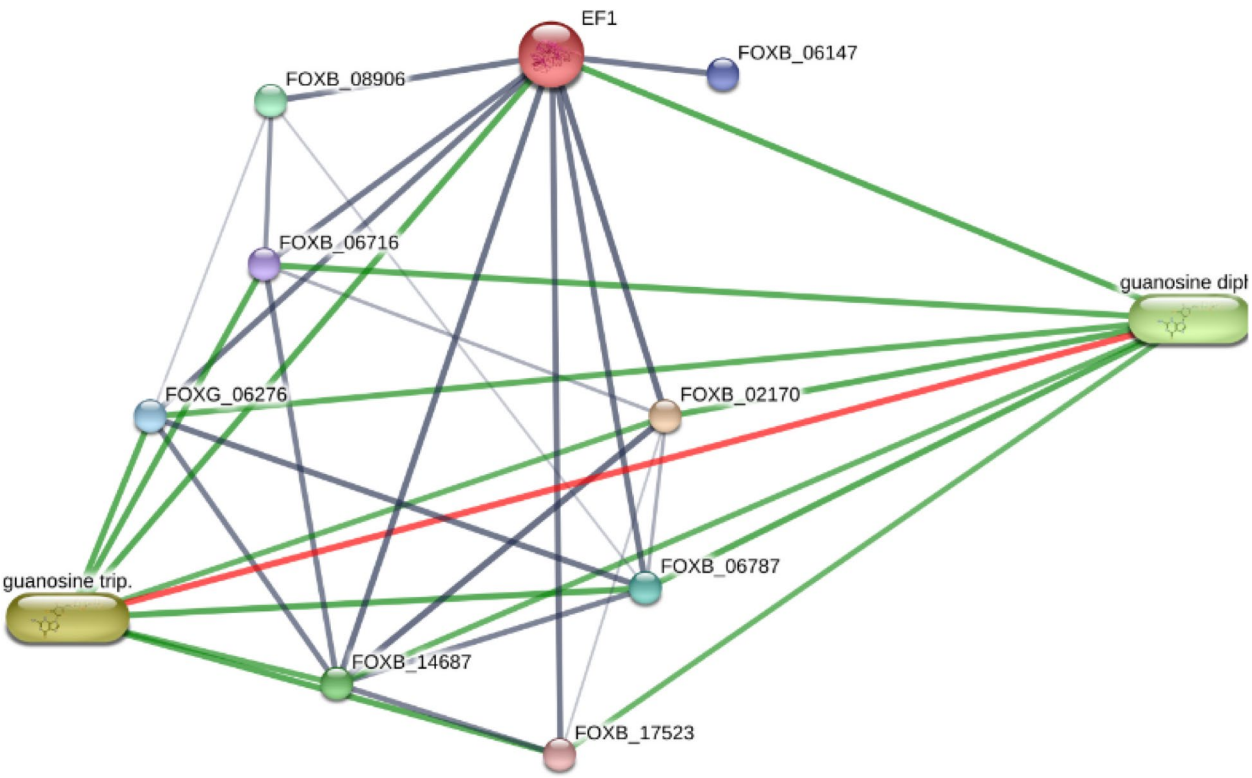

Fig. 8 Predicted *Fusarium oxysporum* elongation factor 1α partners and interaction network. EF1α interacting proteins were screened and the interaction networks were constructed using Chemical-Protein Interaction Networks STITCH database

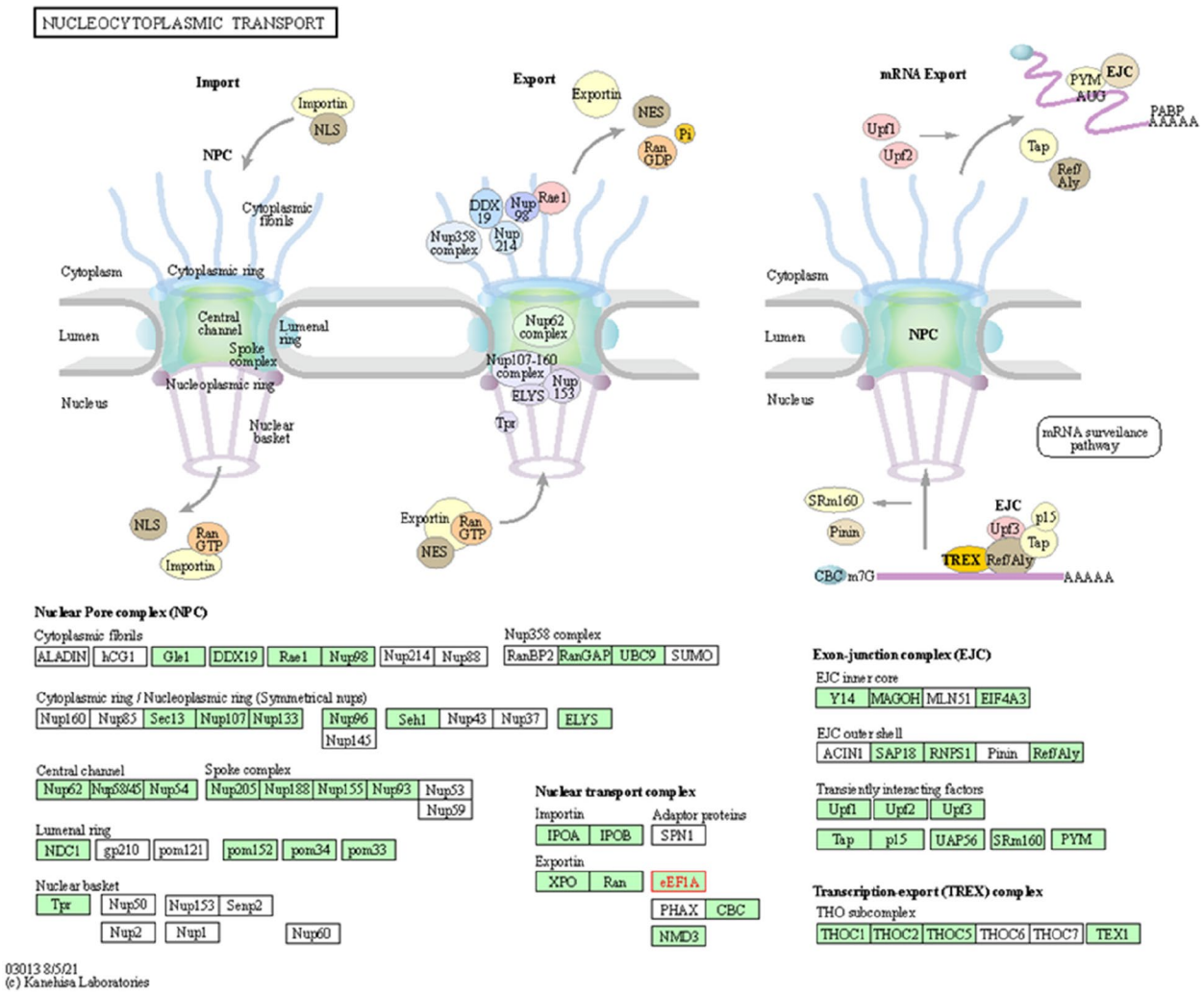

Fig. 9 Picture showing details of EF1α (FOXG_03515) involved in Nucleocytoplasmic transport pathway from *Fusarium oxysporum*

base for prevention, diagnosis and treatment of Fusarium wilt disease in tomato by characterizing features and interacting partners associated with *EF1α* gene of Fol.

The structurally homologous templates of full-length protein (XP_018237716.1) of Fol EF1α were retrieved using BLASTp. The homology modelling was done using template crystal structure of the yeast elongation factor complex EEF1A:EEF1BA (PDB ID: 1F60_A) which showed maximum similarity with the target protein (83.18%). Three-dimensional structure of EF1α was modelled successfully having 95.6% residues in the most favoured region. This indicates better stereochemical quality of the predicted model since the model has > 90% amino acid in the most favoured region [43].

From the Venn diagram, 4 common elements in "MCODE", "CytoHubba" and "CytoNCA" were identified, which are the significant hub genes that are similar between all groups (Fig. 7c). These 4 proteins were 50S ribosomal protein L23Ae (A0A0D2Y2M4), Ribosomal protein L18e/L15P domain-containing protein (A0A0D2XNM9), 40S ribosomal protein S24 (A0A0D2YBR1) and EF1α (A0A0C4DHQ7). The other three proteins were identified as prominent interactors of A0A0C4DHQ7. They can play potential role in fusarium wilt disease management. In previous studies, it has been found that 40S ribosomal proteins play role in regulating virulence ability of disease-causing fungi. PsRPs26, a 40S ribosomal protein regulates growth and pathogenicity of rust causing fungus, *Puccinia striiformis* f. sp. *tritici* [44]. In *Saccharomyces cerevisiae,* pre-40S small ribosomal subunit is synthesised by the ATPase activity of Fap7, an important ribosome assembly factor. MoFap7, a homologous protein of ScFap7 in rice blast causing fungus *M. oryzae* has been reported to play role in development and pathogenesis [45]. The homologs of identified prominent hub genes (A0A0D2Y2M4, A0A0D2XNM9 and A0A0D2YBR1) showed maximum similarity with *Neurospora crassa* ribosome arrested by cycloheximide (PDB

Table 3 Protein-drug interaction analysis using STITCH server

#node1	node2	coexpression	Experimentally determined interaction	Database annotated	Automated text mining	Combined score
FOXB_14687	FOXB_02170	0.76	0.93	0.674	0.538	0.997
guanosine trip	guanosine diph	0	0	0.9	0.962	0.996
EF1	FOXB_02170	0.215	0.762	0.751	0.892	0.994
EF1	guanosine trip	0	0.601	0.867	0.627	0.979
FOXB_06787	guanosine diph	0	0.771	0.867	0.231	0.975
FOXB_06787	guanosine trip	0	0.538	0.867	0.627	0.975
EF1	guanosine diph	0	0.771	0.867	0.197	0.974
EF1	FOXB_14687	0.44	0.836	0.44	0.538	0.973
FOXB_17523	guanosine trip	0	0.69	0.867	0.202	0.965
FOXB_02170	guanosine diph	0	0.771	0.849	0	0.964
FOXB_06716	guanosine trip	0	0.538	0.792	0.627	0.962
FOXG_06276	guanosine trip	0	0.538	0.758	0.596	0.952
FOXB_06716	guanosine diph	0	0.704	0.792	0.231	0.95
FOXB_08906	EF1	0	0.59	0	0.869	0.944
FOXG_06276	FOXB_06787	0	0	0	0	0.943
FOXB_06787	EF1	0.521	0.239	0.448	0.536	0.939
FOXG_06276	EF1	0.521	0.197	0.448	0.536	0.937
FOXG_06276	guanosine diph	0	0.674	0.758	0.231	0.935
FOXB_06147	EF1	0	0.81	0	0.658	0.932
FOXB_06716	EF1	0.521	0.239	0.448	0.536	0.923
EF1	FOXB_17523	0.134	0.638	0.46	0.567	0.917
FOXB_14687	guanosine trip	0	0	0.897	0.107	0.905
FOXB_14687	guanosine diph	0	0	0.897	0	0.897
FOXB_02170	guanosine trip	0	0	0.849	0.234	0.881
FOXG_06276	FOXB_14687	0.785	0	0	0.43	0.872
FOXB_06787	FOXB_14687	0.785	0	0	0.43	0.872
FOXB_06716	FOXB_14687	0.785	0	0	0.43	0.872
FOXB_17523	guanosine diph	0	0	0.867	0	0.867
FOXB_17523	FOXB_14687	0.278	0.656	0	0.474	0.857
FOXB_08906	FOXB_06716	0	0.674	0	0.223	0.735
FOXB_06716	FOXB_02170	0.268	0	0	0.441	0.573
FOXB_06787	FOXB_02170	0.268	0	0	0.441	0.573
FOXB_17523	FOXB_02170	0.169	0.303	0	0.065	0.411
FOXB_08906	FOXB_06787	0	0.27	0	0.223	0.408
FOXB_08906	FOXG_06276	0	0.267	0	0.223	0.406

ID: 7R81). Cycloheximide is a known fungicide that inhibits eukaryotic ribosomes engaged in translation elongation [46]. This study thus proves that the identified targets from Fol, through gene network, cluster and hub gene analysis can be prominent targets to manage wilt disease in tomato caused by Fol.

Mining of proteins that interact with Fol EF1α was done using STITCH database. From the STITCH database analysis, it was found that EF1α and its interacting protein partners also interact with two known chemicals, guanosine diphosphate (GDPNP) and guanosine triphosphate (GTP) (Fig. 8) A homolog of Fol EF1α was identified as Yeast EEF1A:EEF1BA in complex with GDPNP (PDB ID: 1G7C). Further, when Fol EF1α sequence was subjected to NCBI PDB Blast, it was found similar to the crystal structure of *Sulfolobus solfataricus* EF1α in complex with GDP having 94% query coverage and 51.20% identity [47]. These studies suggest that Fol EF1α is structurally similar with yeast and *Sulfolobus solfataricus* which already have a known ligand complex, and that may help in determining their active site cavity for computational screening of fungicides. The other eight proteins that were found to be functional partners of EF1α from STITCH

analysis, they can also be used for protein–ligand interaction study to screen potential fungicides. Thus, the overall study suggests that Fol EF1α and its interacting partners can be used as possible targets for fungicide screening against Fol pathogenesis.

Conclusions

In this study, one cluster with top 10 hub genes (RPS0, A0A0D2YBR1, A0A0D2XMI5, A0A0D2Y2S2, A0A0D2XHU2, A0A0D2XB71, A0A0D2XNM9, A0A0D2Y2M4, A0A0D2XDZ1 and A0A0C4DHQ7) out of which 4 major interactors (A0A0D2Y2M4, A0A0D2XNM9, A0A0D2YBR1 and A0A0C4DHQ7) were identified. KEGG pathway analysis concluded that EF1α is associated with the Nucleocytoplasmic transport pathway (Pathway ID: fox03013). These findings give us fresh insights into potential targets for fungicide development against tomato Fusarium wilt and points towards new possibilities in wilt disease management.

Abbreviations

FW	Fusarium wilt
Fol	*Fusarium oxysporum* f. sp. *lycopersici*
FO	*Fusarium oxysporum*
EF1α	Translation elongation factor 1α
PPIs	Protein-protein interactions
CTAB	Cetyltrimethyl ammonium bromide
MCODE	Molecular Complex Detection
PCI	Protein-chemical interaction

Supplementary Information

The online version contains supplementary material available at https://doi.org/10.1186/s12866-024-03434-x.

Supplementary Material 1.

Supplementary Material 2.

Supplementary Material 3.

Supplementary Material 4.

Supplementary Material 5.

Supplementary Material 6.

Acknowledgements

Yashoda Nandan Tripathi is grateful to the Department of Botany, DST-FIST, DST-PURSE and Interdisciplinary School of Life Sciences (ISLS), Banaras Hindu University, Varanasi, India, for providing various laboratory facilities and thankful to CAS, Centre for Advanced Studies, Department of Botany, Banaras Hindu University for financial assistance.

Authors' contributions

YNT conceptualized, wrote the original draft, curated data and designed the methodology. VKS also helped in designing the methodology and performed investigation. SK, VS and MY have done formal analysis and data interpretation. RSU validated, visualized and supervised the whole study. All authors reviewed the manuscript.

Funding

This research did not receive any specific grant from funding agencies in the public, commercial, or not-for-profit sectors.

Availability of data and materials

All data generated or analysed during this study are included in this published article [and its supplementary information files]. All data is already released and made public. The accession number of the DNA sequence and the protein ID can be found in the supplementary file.

Declarations

Ethics approval and consent to participate

The tomato cultivar (Sel 7) used in the present study complied with local or national guidelines. Taking permission or obtaining license was not required.

Consent for publication

Not applicable.

Competing interests

The authors declare no competing interests.

Author details

[1]Department of Botany, Institute of Science, Banaras Hindu University, Varanasi, Uttar Pradesh, India. [2]School of Biotechnology, Institute of Science, Banaras Hindu University, Varanasi, Uttar Pradesh, India.

Received: 3 June 2023 Accepted: 22 July 2024
Published online: 11 September 2024

References

1. Agrios GN. Plant pathology. San Diego: Academic Press: Elsevier; 2005. https://doi.org/10.1016/C2009-0-02037-6.
2. Nirmaladevi D, Venkataramana M, Srivastava RK, Uppalapati SR, Gupta VK, Yli-Mattila T, et al. Molecular phylogeny, pathogenicity and toxigenicity of Fusarium oxysporum f. sp. lycopersici. Sci Rep. 2016;6:21367. https://doi.org/10.1038/srep21367.
3. Kirankumar R, Jagadeesh K, Krishnaraj P, Patil M. Enhanced growth promotion of tomato and nutrient uptake by plant growth promoting rhizobacterial isolates in presence of tobacco mosaic virus pathogen. Karnataka J Agric Sci. 2010;21(2):309–11.
4. Geiser DM, Aoki T, Bacon CW, Baker SE, Bhattacharyya MK, Brandt ME, et al. One fungus, one name: defining the genus Fusarium in a scientifically robust way that preserves longstanding use. Phytopathology. 2013;103(5):400–8. https://doi.org/10.1094/phyto-07-12-0150-le.
5. Zuriegat Q, Zheng Y, Liu H, Wang Z, Yun Y. Current progress on pathogenicity-related transcription factors in Fusarium oxysporum. Mol Plant Pathol. 2021;22(7):882–95. https://doi.org/10.1111/mpp.13068.
6. Takken F, Rep M. The arms race between tomato and Fusarium oxysporum. Mol Plant Pathol. 2010;11(2):309–14. https://doi.org/10.1111/j.1364-3703.2009.00605.x.
7. Di X, Cao L, Hughes RK, Tintor N, Banfield MJ, Takken FLW. Structure-function analysis of the Fusarium oxysporum Avr2 effector allows uncoupling of its immune-suppressing activity from recognition. New Phytol. 2017;216(3):897–914. https://doi.org/10.1111/nph.14733.
8. Pietro AD, Madrid MP, Caracuel Z, Delgado-Jarana J, Roncero MI. Fusarium oxysporum: exploring the molecular arsenal of a vascular wilt fungus. Mol Plant Pathol. 2003;4(5):315–25. https://doi.org/10.1046/j.1364-3703.2003.00180.x.
9. Raja HA, Miller AN, Pearce CJ, Oberlies NH. Fungal identification using molecular tools: a primer for the natural products research community. J Nat Prod. 2017;80(3):756–70. https://doi.org/10.1021/acs.jnatprod.6b01085.
10. Boutigny AL, Gautier A, Basler R, Dauthieux F, Leite S, Valade R, et al. Metabarcoding targeting the EF1 alpha region to assess Fusarium diversity on cereals. PLoS One. 2019;14(1):e0207988. https://doi.org/10.1371/journal.pone.0207988.
11. O'Donnell K, Ward TJ, Aberra D, Kistler HC, Aoki T, Orwig N, et al. Multilocus genotyping and molecular phylogenetics resolve a novel head blight pathogen within the Fusarium graminearum species complex

from Ethiopia. Fungal Genet Biol. 2008;45(11):1514–22. https://doi.org/10.1016/j.fgb.2008.09.002.
12. Sprinzl M. Elongation factor Tu: a regulatory GTPase with an integrated effector. Trends Biochem Sci. 1994;19(6):245–50. https://doi.org/10.1016/0968-0004(94)90149-X.
13. Harvey KL, Jarocki VM, Charles IG, Djordjevic SP. The diverse functional roles of elongation factor Tu (EF-Tu) in microbial pathogenesis. Front Microbiol. 2019;10:2351. https://doi.org/10.3389/fmicb.2019.02351.
14. Prezioso SM, Brown NE, Goldberg JB. Elfamycins: Inhibitors of elongation factor-Tu. Mol Microbiol. 2017;106(1):22–34. https://doi.org/10.1111/mmi.13750.
15. Wolf H, Chinali G, Parmeggiani A. Kirromycin, an inhibitor of protein biosynthesis that acts on elongation factor Tu. Proc Natl Acad Sci. 1974;71(12):4910–4. https://doi.org/10.1073/pnas.71.12.491.
16. Yoon J-H, Ryu J, Baek SJ. Moonlighting activity of secreted inflammation-regulatory proteins. Yonsei Med J. 2018;59(4):463. https://doi.org/10.3349/ymj.2018.59.4.463.
17. Min K-W, Lee S-H, Baek SJ. Moonlighting proteins in cancer. Cancer Lett. 2016;370(1):108–16. https://doi.org/10.1016/j.canlet.2015.09.022.
18. Petit FM, Serres C, Auer J. Moonlighting proteins in sperm–egg interactions. Biochem Soc Trans. 2014;42(6):1740–3. https://doi.org/10.1042/BST20140218.
19. Huberts DH, van dervan Klei IJ. Moonlighting proteins: an intriguing mode of multitasking. Biochim Biophys Acta. 2010;1803(4):520–5. https://doi.org/10.1016/j.bbamcr.2010.01.022.
20. Jeffery CJ. Moonlighting proteins. Trends Biochem Sci. 1999;24(1):8–11. https://doi.org/10.1016/S0968-0004(98)01335-8.
21. Liu H, Lu X, Li M, Lun Z, Yan X, Yin C, et al. Plant immunity suppression by an exo-β-1, 3-glucanase and an elongation factor 1α of the rice blast fungus. Nat Commun. 2023;14(1):5491. https://doi.org/10.1038/s41467-023-41175-z.
22. Farooq QUA, Shaukat Z, Aiman S, Li CH. Protein-protein interactions: Methods, databases, and applications in virus-host study. World J Virol. 2021;10(6):288–300. https://doi.org/10.5501/wjv.v10.i6.288.
23. Gonzalez MW, Kann MG. Chapter 4: protein interactions and disease. PLoS Comput Biol. 2012;8(12):e1002819. https://doi.org/10.1371/journal.pcbi.1002819.
24. Zahiri J, Hannon Bozorgmehr J, Masoudi-Nejad A. Computational prediction of protein–protein interaction networks: algorithms and resources. Curr Genomics. 2013;14(6):397–414. https://doi.org/10.2174/1389202911314060004.
25. Singh VK, Upadhyay RS. Fusaric acid induced cell death and changes in oxidative metabolism of Solanum lycopersicum L. Bot Stud. 2014;55(1):66. https://doi.org/10.1186/s40529-014-0066-2.
26. Catanzariti AM, Lim GTT, Jones DA. The tomato I-3 gene: a novel gene for resistance to Fusarium wilt disease. New Phytol. 2015;207(1):106–18. https://doi.org/10.1111/nph.13348.
27 Wang M, Ling N, Dong X, Zhu Y, Shen Q, Guo S. Thermographic visualization of leaf response in cucumber plants infected with the soil-borne pathogen Fusarium oxysporum f. sp. cucumerinum. Plant Physiol Biochem. 2012;61:153–61. https://doi.org/10.1016/j.plaphy.2012.09.015.
28. Möller EM, Bahnweg G, Sandermann H, Geiger HH. A simple and efficient protocol for isolation of high molecular weight DNA from filamentous fungi, fruit bodies, and infected plant tissues. Nucleic Acids Res. 1992;20(22):6115–6. https://doi.org/10.1093/nar/20.22.6115.
29. Liu X, Xing M, Kong C, Fang Z, Yang L, Zhang Y, et al. Genetic diversity, virulence, race profiling, and comparative genomic analysis of the Fusarium oxysporum f. sp. conglutinans strains infecting cabbages in China. Front Microbiol. 2019;10:1373. https://doi.org/10.3389/fmicb.2019.01373.
30. O'Donnell K, Kistler HC, Cigelnik E, Ploetz RC. Multiple evolutionary origins of the fungus causing Panama disease of banana: concordant evidence from nuclear and mitochondrial gene genealogies. Proc Natl Acad Sci U S A. 1998;95(5):2044–9. https://doi.org/10.1073/pnas.95.5.2044.
31. Tamura K, Stecher G, Kumar S. MEGA11: molecular evolutionary genetics analysis version 11. Mol Biol Evol. 2021;38(7):3022–7. https://doi.org/10.1093/molbev/msab120.
32. Altschul SF, Madden TL, Schäffer AA, Zhang J, Zhang Z, Miller W, et al. Gapped BLAST and PSI-BLAST: a new generation of protein database search programs. Nucleic Acids Res. 1997;25(17):3389–402. https://doi.org/10.1093/nar/25.17.3389.
33 Johnson M, Zaretskaya I, Raytselis Y, Merezhuk Y, McGinnis S, Madden TL. NCBI BLAST: a better web interface. Nucleic Acids Res. 2008;36(Web Server issue):W5–9. https://doi.org/10.1093/nar/gkn201.
34. Laskowski RA, Hutchinson EG, Michie AD, Wallace AC, Jones ML, Thornton JM. PDBsum: a Web-based database of summaries and analyses of all PDB structures. Trends Biochem Sci. 1997;22(12):488–90. https://doi.org/10.1016/s0968-0004(97)01140-7.
35. Szklarczyk D, Gable AL, Nastou KC, Lyon D, Kirsch R, Pyysalo S, et al. The STRING database in 2021: customizable protein-protein networks, and functional characterization of user-uploaded gene/measurement sets. Nucleic Acids Res. 2021;49(D1):D605–12. https://doi.org/10.1093/nar/gkaa1074.
36. Shannon P, Markiel A, Ozier O, Baliga NS, Wang JT, Ramage D, et al. Cytoscape: a software environment for integrated models of biomolecular interaction networks. Genome Res. 2003;13(11):2498–504. https://doi.org/10.1101/gr.1239303.
37 Chin CH, Chen SH, Wu HH, Ho CW, Ko MT, Lin CY. cytoHubba: identifying hub objects and sub-networks from complex interactome. BMC Syst Biol. 2014;8 Suppl 4(Suppl 4):S11. https://doi.org/10.1186/1752-0509-8-s4-s11.
38 Kuhn M, von Mering C, Campillos M, Jensen LJ, Bork P. STITCH: interaction networks of chemicals and proteins. Nucleic Acids Res. 2008;36(Database issue):D684–8. https://doi.org/10.1093/nar/gkm795.
39. Tang Y, Li M, Wang J, Pan Y, Wu FX. CytoNCA: a cytoscape plugin for centrality analysis and evaluation of protein interaction networks. Biosystems. 2015;127:67–72. https://doi.org/10.1016/j.biosystems.2014.11.005.
40. Terry LJ, Shows EB, Wente SR. Crossing the nuclear envelope: hierarchical regulation of nucleocytoplasmic transport. Science. 2007;318(5855):1412–6. https://doi.org/10.1126/science.1142204.
41. Mirhendi H, Makimura K, de Hoog GS, Rezaei-Matehkolaei A, Najafzadeh MJ, Umeda Y, et al. Translation elongation factor 1-α gene as a potential taxonomic and identification marker in dermatophytes. Med Mycol. 2015;53(3):215–24. https://doi.org/10.1093/mmy/myu088.
42. Aamir M, Singh VK, Dubey MK, Meena M, Kashyap SP, Katari SK, et al. In silico prediction, characterization, molecular docking, and dynamic studies on fungal SDRs as novel targets for searching potential fungicides against Fusarium wilt in tomato. Front Pharmacol. 2018;9:1038. https://doi.org/10.3389/fphar.2018.01038.
43. Rai DK, Rieder E. Homology modeling and analysis of structure predictions of the bovine rhinitis B virus RNA dependent RNA polymerase (RdRp). Int J Mol Sci. 2012;13(7):8998–9013. https://doi.org/10.3390/ijms13078998.
44 Wang B, Song N, Tang C, Ma J, Wang N, Sun Y, et al. PsRPs26, a 40S ribosomal protein subunit, regulates the growth and pathogenicity of puccinia striiformis f. sp. Tritici. Front Microbiol. 2019;10:968. https://doi.org/10.3389/fmicb.2019.00968.
45. Li L, Zhu XM, Shi HB, Feng XX, Liu XH, Lin FC. MoFap7, a ribosome assembly factor, is required for fungal development and plant colonization of Magnaporthe oryzae. Virulence. 2019;10(1):1047–63. https://doi.org/10.1080/21505594.2019.1697123.
46. Shen L, Su Z, Yang K, Wu C, Becker T, Bell-Pedersen D, et al. Structure of the translating Neurospora ribosome arrested by cycloheximide. Proc Natl Acad Sci U S A. 2021;118(48):e2111862118. https://doi.org/10.1073/pnas.2111862118.
47. Vitagliano L, Masullo M, Sica F, Zagari A, Bocchini V. The crystal structure of Sulfolobus solfataricus elongation factor 1alpha in complex with GDP reveals novel features in nucleotide binding and exchange. Embo j. 2001;20(19):5305–11. https://doi.org/10.1093/emboj/20.19.5305.

Publisher's Note